Nomenclature

IMM	Interacting multiple model
EKF	extended Kalman filter
CV	Constant velocity model
CA	Constant acceleration model
CJ	Constant jerk model
X,Y, Z	Coordinates in Cartesian frame
k	time instant
$M_j(k)$	j^{th} model at k^{th} instant
$X(k)$	state vector at k^{th} instant
$P(k)$	state covariance matrix
$\hat{X}(k \mid k)$	estimated state vector
$\hat{P}(k \mid k)$	estimated state covariance matrix
$\tilde{X}(k \mid k-1)$	predicted state vector
$\tilde{P}(k \mid k-1)$	predicted state covariance matrix
$k \mid k-1$	$(k-1)^{th}$ instant to k^{th} instant
Φ_j	state transition matrix at j^{th} model
w_j	process noise of the j^{th} model
v_j	measurement noise of the j^{th} model
$Z(k)$	measurement vector at k^{th} instant
H_j	measurement/observation matrix for the j^{th} model
P_{0j}	mixed state covariance matrix for the j^{th} model
X_{0j}	mixed state vector for the j^{th} model
Q_j	model process noise covariance matrix for the j^{th} model
R	measurement noise covariance matrix
r	number of models
$\mu_{i\mid j}$	mixing probability

μ_j	predicted mode probability for the j^{th} model
G_j	process noise gain matrix for the j^{th} model
S_j	innovation covariance matrix for the j^{th} model
K_j	Kalman gain for the j^{th} model
υ_j	innovation sequence for the j^{th} model
Λ_j	likelihood function for the j^{th} model
p_{ij}	mode transition probability
T	sampling interval
ρ	range
θ	azimuth
ϕ	elevation
$x(k)$	target x-position at k^{th} instant
$y(k)$	target y-position at k^{th} instant
$z(k)$	target z-position at k^{th} instant
$\tilde{z}_j(k \mid k-1)$	predicted measurement for the j^{th} model
$h(X)$	nonlinear function on states
PFE	Percentage fit error
$RMSPE$	root mean square position error
$RMSVE$	root mean square velocity error
$RMSAE$	root mean square acceleration error
$RSSPE$	root sum square position error
$RSSVE$	root sum square velocity error
$RSSAE$	root sum square acceleration error
X_{true}	true state vector
$\hat{x}$	estimated x-position state, similarly for y- and z-position
$\dot{x}$	x-velocity state, (y- and z-velocity states)
$\ddot{x}$	x-acceleration state, (y- and z-acceleration states)
$\dddot{x}$	x-jerk sate, (y- and z-jerk states)

$\hat{\dot{x}}$ estimated x-velocity state, (y- and z-velocity states)

$\hat{\ddot{x}}$ estimated x-acceleration state, (y- and z-accleration states)

$\hat{\dddot{x}}$ estimated x-jerk state, (y- and z-jerk states)

N number of data points

$\sigma_\rho, \sigma_\theta, \sigma_\phi$ noise standard deviation for the range, the azimuth and the elevation

σ_x^2 x position process noise variance

σ_y^2 y position process noise variance

σ_z^2 z position process noise variance

n dimension of innovation sequence

$Pr\{.\}$ probability of an event

c normalization factor

Q_1, Q_2, Q_3 process noise covariance matrices for constant velocity, constant acceleration and constant jerk models

Φ_1, Φ_2, Φ_3 state transition matrices for velocity model, acceleration model and jerk model

1. Introduction

Kalman filter which is used extensively in target tracking applications performs optimally when the model describing the target motion is specified correctly. In tracking applications, for targets moving with constant velocity (CV), the state model includes the first derivative of position and for targets moving with constant acceleration (CA) it includes second derivative of position[1]. Models with second order derivatives are preferred for tracking maneuvering targets and referred to as acceleration models[2,3]. However, for highly maneuvering targets, it is seen[4] that the tracking performance of acceleration model is not very accurate since under large maneuver conditions, higher order derivatives of position become significant. Hence, models which include third order derivative of the target position, termed constant jerk (CJ) models are preferred for tracking targets executing evasive maneuvers[4].

Jerk is the time derivative of acceleration. In most coordinate uncoupled models, the target acceleration is chosen to be the descriptor of a target maneuver and modeled as a random process or as a first order Gauss Markov process[5]. Since acceleration is directly related to the force acting on the target and causing the maneuver, it is usually taken to be the control input to the state model. However, for agile targets, it may be convenient to use a random jerk process to model the target maneuvers[6]. A jerk model differs from an acceleration model in that the target motion is better described by a random process model of the jerk rather than the acceleration. However, the estimation accuracy of jerk is usually poorer than acceleration estimates as only position measurements are available.

Tracking a randomly maneuvering target with highly time varying and uncertain dynamics requires an adaptive state estimation. Interacting Multiple Model (IMM) Kalman filter[2,3,7] is one such adaptive estimator which is based on the assumption that a finite number of models are required to characterize the target motion at all times. To the authors knowledge, the usage of CJ model in IMM estimator for tracking highly maneuvering targets is not available in open literature. In this paper CJ model is used as one of the models of IMM for tracking randomly maneuvering target. To bring out the benefits of inclusion of CJ model in IMM estimator following cases have been studied using simulated data of a target executing evasive/agile maneuver in the Cartesian X-Z plane as observed by a ground based radar.

(i) Kalman filter with only CA model

(ii) Kalman filter with only CJ model

(iii) IMM Kalman filter with CV and CA models

(iv) IMM Kalman filter with CV and CJ models

(v) IMM Kalman filter with CV, CA and CJ models

The two model IMMKF algorithm is presented in Section 2 with relevant equations to show its mechanism of selecting the model corresponding to each behavior mode of the target and simultaneous estimation of target states. Different tracking models, CV, CA and CJ are described in Section 3. The measurements available from the ground based radar are noisy range, azimuth and elevation. The target tracking is carried out in three dimensional Cartesian coordinate system. The states include position, velocity, acceleration and jerk components in the Cartesian XYZ coordinate system. The radar measurements of range, azimuth and elevation are non linear functions of the states, necessitating the use of EKF in IMM. For validation of the IMM algorithm with different combination of models, a typical maneuver target motion is simulated with a resultant 9g acceleration in Cartesian X-Z plane. Results of tracking the target from this simulated data using IMMKF with different combination of models are presented in terms of, percentage fit error of the estimated states w.r.t true states, root sum square and root mean square position, velocity and acceleration errors and autocorrelation of residuals with their theoretical bounds. Ground based radar tracking the roller coaster maneuver target is also generated using ELS facility at FMCD, NAL to evaluate the performance of IMM algorithm with and without jerk model. All the results presented in the paper are the average of 100 Monte Carlo simulations.

2. Interacting Multiple Model Algorithm

IMM is a sub-optimal hybrid estimator since it is characterized by both continuous valued parameters like target position, velocity, acceleration and jerk defined by the difference or differential form of state equations, as well as by the discrete stochastic process that controls the selection of a model corresponding to each behavior mode. The IMM, thus, performs both target state estimation as well as model selection from a given set of models. The “model set” may consist of several models, such as CV model, CA model, CJ model, coordinated turn model, etc. A finite state Markov chain with known transition probabilities is used to switch from one model to another. The mode transition probabilities, which constitute the transition matrix, are the design parameters for the algorithm. Initial mode probabilities are generally selected on the basis that a target is more likely to be in non-maneuver mode than in maneuver mode. Thus, the IMM algorithm, in general, consists of a set of model matched filter modules that interact in certain way to yield the mode-conditioned state estimates. The individual mode matched filters can either be Kalman Filters (KF) or Extended Kalman Filters (EKF).

Let us consider $M_1, M_2, M_3, ..., M_r$ as the r models of IMMKF and let $M_j(k)$ mean that the model M_j is in effect during the sampling period ending at frame k. During the event $M_j(k+1)$ the state of the target evolves according to the following equation:

$$X(k+1) = \Phi_j X(k) + G_j w_j(k) \tag{1}$$

with the measurement given by:

$$Z(k+1) = HX(k+1) + v(k+1) \tag{2}$$

where Φ_j is the transition matrix and H_j is the measurement matrix for $M_j(k+1)$. The process noise $w_j(k)$ and the measurement noise $v_j(k)$ are zero-mean, mutually independent, white, Gaussian processes with covariance matrices $Q_j(k)$ and $R(k)$ respectively. Figure 1 shows the block diagram of IMMKF. For simplicity, two model IMMKF is considered i.e. $r = 2$ and $j = 1$ to r, estimation with more than two models poses no problem and can be extended easily.

The IMMKF algorithm has following four major steps.

2.1 Interaction/mixing:

For the event $M_j(k+1)$, the mixed estimate $X_{0j}(k|k)$ and the covariance $P_{0j}(k|k)$ are computed as

$$\hat{X}_{0j}(k \mid k) = \sum_{i=1}^{r} \mu_{i|j}(k \mid k)\, \hat{X}_i(k \mid k)$$
$$\hat{P}_{0j(k|k)} = \sum_{i=1}^{r} \mu_{i|j(k|k)} \left\{ \hat{P}_i(k|k) + \left[\hat{X}_i(k|k) - \hat{X}_{0j}(k|k) \right] \left[\hat{X}_i(k|k) - \hat{X}_{0j(k|k)} \right]^T \right\} \tag{3}$$

The mixing probabilities $\mu_{i|j}(k \mid k)$ are given by

$$\mu_{i|j}(k|k) = \frac{1}{\mu_{j(k+1|k)}} \; p_{ij} \; \mu_i(k|k) \tag{4}$$

where the predicted mode probability $\mu_{j(k+1|k)}$ is computed by

$$\mu_{j(k+1|k)} = \sum_{i=1}^{r} p_{ij} \; \mu_i(k|k) \tag{5}$$

The mode switching process (usually Markov process) is specified by the following mode transition probabilities

$$p_{ij} = Pr\left\{ M_{j(k+1)} \mid M_i(k) \right\} \tag{6}$$

Where $Pr\{.\}$ denotes the probability of an event, which means p_{ij} is the probability that M_i model at kth instant is switching over to M_j model at (k+1)th instant.

2.2 Kalman filtering:

The usual Kalman filter equations are used with appropriate target motion models to update the mixed state estimates with current measurement. In case of a nonlinear state or measurement equations, extended Kalman filter formulation will be used. Separate filters are used for each mode.

In each filter, the time update part consists of the following equations.

Predicted state: $$\tilde{X}_j(k+1 \mid k) = \Phi_j \hat{X}_{0j}(k \mid k) \tag{7}$$

Predicted measurement: $$\tilde{z}_j(k+1 \mid k) = H_j \tilde{X}_j(k+1 \mid k) \tag{8}$$

Predicted state covariance: $$\tilde{P}_j(k+1 \mid k) = \Phi_j \hat{P}_{0j}(k \mid k)(\Phi_j)^T + G_j Q_j(k) G_j^T \tag{9}$$

Innovation covariance: $$S_j(k+1) = H_j \tilde{P}_j(k+1 \mid k) H_j^T + R(k+1) \tag{10}$$

The measurement update part consists of the following equations.

Filter gain: $$K_j(k+1) = \tilde{P}_j(k+1|k) H_j^T \left(S_j(k+1)\right)^{-1} \quad (11)$$

Innovation: $$\upsilon_j(k+1) = z(k+1) - \tilde{z}_j(k+1|k) \quad (12)$$

Updated state estimate: $$\hat{X}_j(k+1 \mid k+1) = \tilde{X}_j(k+1 \mid k) + K_j(k+1)\upsilon_j(k+1) \quad (13)$$

Updated state covariance: $$\hat{P}_j(k+1 \mid k+1) = \left[I - K_j(k+1)H_j\right]\tilde{P}_j(k+1|k) \quad (14)$$

The likelihood function for matched filter j is a Guassian density function of innovation $\upsilon_{j\,(k+1)}$ with zero mean and covariance $S_{j\,(k+1)}$. It is computed as

$$\Lambda_{j\,(k+1)} = \frac{1}{(2\Pi)^{n/2}\sqrt{\left|S_{j\,(k+1)}\right|}} exp\left\{-\frac{1}{2}(\upsilon_{j\,(k+1)})^T (S_{j\,(k+1)})^{-1} \upsilon_{j\,(k+1)}\right\} \quad (15)$$

where n denotes the dimension of the innovation vector υ.

2.3 Mode probability update:

After each model has been updated with measurement $z_{(k+1)}$, the mode probability $\mu_{j\,(k+1|k+1)}$ is updated using likelihoods $\Lambda_{j\,(k+1)}$ and the predicted mode probabilities $\mu_{j\,(k+1|k)}$ for $M_{j\,(k+1)}$.

$$\mu_{j\,(k+1|k+1)} = \frac{1}{c}\mu_{j\,(k+1|k)}\Lambda_{j\,(k+1)} \quad (16)$$

where the normalization factor $c = \sum_{i=1}^{r} \mu_{i\,(k+1|k)}\Lambda_{i\,(k+1)}$ (17)

2.4 State estimate combiner:

Finally the estimated states $\hat{X}_j(k+1 \mid k+1)$ and covariance $\hat{P}_j(k+1 \mid k+1)$ from each filter are combined using the updated mode probability $\mu_j(k+1 \mid k+1)$ to produce overall state estimate $\hat{X}(k+1 \mid k+1)$ and the associated covariance $\hat{P}(k+1 \mid k+1)$ as given below:

$$\hat{X}(k+1\,|\,k+1) = \sum_{j=1}^{r} \mu_{j(k+1|k+1)} \hat{X}_j(k+1\,|\,k+1)$$

$$\hat{P}(k+1\,|\,k+1) = \sum_{j=1}^{r} \mu_j(k+1\,|\,k+1) \left\{ \begin{aligned} &\hat{P}_j(k+1\,|\,k+1) + \\ &\left[\hat{X}_j(k+1\,|\,k+1) - \hat{X}(k+1\,|\,k+1)\right]\left[\hat{X}_j(k+1\,|\,k+1) - \hat{X}(k+1\,|\,k+1)\right]^T \end{aligned} \right\} \tag{18}$$

3. Target Motion Models

In this study, following three types of motion models in Cartesian frame are considered for tracking the target.

1. CV model (2^{nd} order kinematic model with position and velocity states)
2. CA model (3^{rd} order kinematic model with position, velocity and acceleration states)
3. CJ model (4^{th} order kinematic model with position, velocity, acceleration and jerk states)

3.1 State Model

The kinematic state model of the target motion is expressed in the form given in equation (1).

3.1.1 Constant Velocity Model

It is a 2DOF kinematic model, with position and velocity components in each of the three Cartesian coordinates X, Y and Z. It has the following transition and process noise gain matrices:

$$\Phi_1 = \Phi_{CV} = \begin{bmatrix} \Phi_V & 0_{4x4} & 0_{4x4} \\ 0_{4x4} & \Phi_V & 0_{4x4} \\ 0_{4x4} & 0_{4x4} & \Phi_V \end{bmatrix} \quad G_1 = G_{CV} = \begin{bmatrix} \varsigma_V & 0_{4x1} & 0_{4x1} \\ 0_{4x1} & \varsigma_V & 0_{4x1} \\ 0_{4x1} & 0_{4x1} & \varsigma_V \end{bmatrix} \tag{20}$$

where

$$\Phi_V = \begin{bmatrix} 1 & T & 0 & 0 \\ 0 & 1 & 0 & 0 \\ 0 & 0 & 0 & 0 \\ 0 & 0 & 0 & 0 \end{bmatrix} \quad \varsigma_V = \begin{bmatrix} \frac{T^2}{2} \\ T \\ 0 \\ 0 \end{bmatrix} \quad 0_{4x4} = \begin{bmatrix} 0 & 0 & 0 & 0 \\ 0 & 0 & 0 & 0 \\ 0 & 0 & 0 & 0 \\ 0 & 0 & 0 & 0 \end{bmatrix} \quad 0_{4x1} = \begin{bmatrix} 0 \\ 0 \\ 0 \\ 0 \end{bmatrix}$$

The state vector in CV model is given by $X = [x \ \dot{x} \ 0 \ 0 \ y \ \dot{y} \ 0 \ 0 \ z \ \dot{z} \ 0 \ 0]$. The process noise intensity which is meant to account for air turbulence, slow turns, and small linear acceleration in each axis is generally assumed to be small and equal in all three axis ($\sigma_X^2 = \sigma_Y^2 = \sigma_Z^2$). It should be noted that the acceleration and jerk components in the above model, though identically equal to zero, have been retained for dimensional compatibility with the 4th order jerk model.

3.1.2 Constant Acceleration Model

It is a 3DOF model, with position, velocity and acceleration components in each of the three Cartesian axes X, Y and Z. It has the following transition and process noise gain matrices:

$$\Phi_2 = \Phi_{CA} = \begin{bmatrix} \Phi_a & 0_{4x4} & 0_{4x4} \\ 0_{4x4} & \Phi_a & 0_{4x4} \\ 0_{4x4} & 0_{4x4} & \Phi_a \end{bmatrix} \quad G_2 = G_{CA} = \begin{bmatrix} \varsigma_a & 0_{4x1} & 0_{4x1} \\ 0_{4x1} & \varsigma_a & 0_{4x1} \\ 0_{4x1} & 0_{4x1} & \varsigma_a \end{bmatrix} \tag{21}$$

where

$$\Phi_a = \begin{bmatrix} 1 & T & \frac{T^2}{2} & 0 \\ 0 & 1 & T & 0 \\ 0 & 0 & 1 & 0 \\ 0 & 0 & 0 & 0 \end{bmatrix} \quad \varsigma_a = \begin{bmatrix} \frac{T^3}{6} \\ \frac{T^2}{2} \\ T \\ 0 \end{bmatrix}$$

The state vector in CA model is given by $X = [x \ \dot{x} \ \ddot{x} \ 0 \ y \ \dot{y} \ \ddot{y} \ 0 \ z \ \dot{z} \ \ddot{z} \ 0]$. A moderate value of process noise variance Q_a (but relatively higher than Q_v) will yield nearly a constant acceleration motion. The noise variances in each coordinate are assumed to be equal ($\sigma_X^2 = \sigma_Y^2 = \sigma_Z^2$).

3.1.3 Constant Jerk Model

It is a 4DOF model, with position, velocity, acceleration and jerk components in each of the three Cartesian coordinates X, Y and Z. It has the following transition and process noise gain matrices:

$$\Phi_3 = \Phi_{CJ} = \begin{bmatrix} \Phi_{jr} & 0_{4x4} & 0_{4x4} \\ 0_{4x4} & \Phi_{jr} & 0_{4x4} \\ 0_{4x4} & 0_{4x4} & \Phi_{jr} \end{bmatrix} \quad G_3 = G_{CJ} = \begin{bmatrix} \varsigma_{jr} & 0_{4x1} & 0_{4x1} \\ 0_{4x1} & \varsigma_{jr} & 0_{4x1} \\ 0_{4x1} & 0_{4x1} & \varsigma_{jr} \end{bmatrix} \tag{22}$$

where

$$\Phi_{jr} = \begin{bmatrix} 1 & T & \frac{T^2}{2} & \frac{T^3}{6} \\ 0 & 1 & T & \frac{T^2}{2} \\ 0 & 0 & 1 & T \\ 0 & 0 & 0 & 1 \end{bmatrix} \quad \varsigma_{jr} = \begin{bmatrix} \frac{T^4}{24} \\ \frac{T^3}{6} \\ \frac{T^2}{2} \\ T \end{bmatrix}$$

The state vector in CJ model is given by $X = [x\ \dot{x}\ \ddot{x}\ \dddot{x}\ \ y\ \dot{y}\ \ddot{y}\ \dddot{y}\ z\ \dot{z}\ \ddot{z}\ \dddot{z}]$. Moderately higher value of process noise variance Q_{jr} (relatively higher than Q_a) will yield nearly a constant jerk motion.

3.2 Measurement Model

The measurement vector of the radar is noisy range (ρ), azimuth (θ) and elevation (ϕ). They are related to states in a nonlinear relationship as given below.

$$\begin{aligned} x(k) &= \rho(k)\ \cos\phi(k)\ \cos\theta(k) \\ y(k) &= \rho(k)\ \cos\phi(k)\ \sin\theta(k) \\ z(k) &= \rho(k)\ \sin\phi(k) \end{aligned} \tag{23}$$

The measurement equation is in the form:

$$Z(k+1) = h(\tilde{X}(k+1)) + v(k+1) \tag{24}$$

where $h(\tilde{X}(k+1))$ is the nonlinear function relating states to measurement. The linearised H matrix required in the Kalman filter is obtained using finite difference method

4. Radar Data Simulation

4.1 Data Set 1

The target motion is simulated with a 9g jerk maneuver in X-Z plane. The target motion trajectory is simulated first in Cartesian coordinates, with a sampling time = 0.025 seconds, using CV model for the first 5 seconds followed by CJ model for the next 3.75 seconds, CA model for the next 6.25 seconds and then CJ model for the 3.27 seconds and CV model for 6.25 seconds. The target acceleration profiles of the target in X and Z axis are shown in figure 2(a). The noisy radar data of target range, azimuth and elevation is then obtained from the following transformations:

$$\begin{aligned}
\rho(k) &= \sqrt{x^2(k)+y^2(k)+z^2}(k)+v_\rho(k) \\
\theta(k) &= tan^{-1}\left(\frac{y(k)}{x(k)}\right)+v_\theta(k) \\
\phi(k) &= tan^{-1}\left(\frac{z(k)}{\sqrt{x^2(k)+y^2(k)}}\right)+v_\phi(k)
\end{aligned} \tag{25}$$

The standard deviation of measurement noise is chosen as : $\sigma_\rho = 50$ m, $\sigma_\theta = \sigma_\phi = 0.5$ deg.

The measurement noise values chosen are representative values from similar simulations in literature [4]. The resultant noisy radar measurements are shown in the figure 2(b).

4.2 Data Set 2

The roller-coaster maneuver data of a fighter aircraft is generated using the 6 degree of freedom engineer in the loop flight simulator. This maneuver has been chosen since this is representative of a target maneuver which if initiated at the proper time could induce large miss distance for the interceptor. Figure 3(a) shows the acceleration profile of aircraft in its body axis.

The 6 degree of freedom simulated data of a fighter aircraft executing roller-coaster maneuver is appropriately transformed to a position data from a fictitious radar station. Then the radar measurements r, θ, φ for tracking the target undergoing rollercoaster maneuver is generated with all the radar characteristics. Figure 3(b) shows the range, azimuth, elevation and their rates as generated by the ground based radar with the noise covariance values as:

Measurement noise = 10 m^2 in range
10^{-6} rad^2 in azimuth
10^{-6} rad^2 in elevation

5. Results and Discussions

To bring out the benefits of inclusion of CJ model in IMM estimator following cases have been studied with the above two sets of simulated tracking radar data:

(i) EKF with only CA model described in equation (20)
(ii) EKF with only CJ model described in equation (22)
(iii) 2-model IMM EKF with CV and CA models described in equations (20) and (21)
(iv) 2-model IMM EKF with CV and CJ models described in equations (20) and (22)
(v) 3-model IMM EKF with CV, CA and CJ models described in equations (20), (21) and (22)

Performance of the filter in each case is evaluated in terms of:

(i) Percentage fit error $\left(PFE = \frac{norm\left(X_{true} - \hat{X}\right)}{norm\left(X_{true}\right)} * 100 \right)$ in position, velocity and acceleration in Cartesian frame. This is possible since true values of position, velocity and acceleration in Cartesian frame are available from simulation.

(ii) Root mean square position error:

$$RMS\,PE = \sqrt{\frac{1}{N}\sum_{k=1}^{N}\frac{\left(x_{true}(k)-\hat{x}(k)\right)^2+\left(y_{true}(k)-\hat{y}(k)\right)^2+\left(z_{true}(k)-\hat{z}(k)\right)^2}{3}}$$

Root mean square velocity error:

$$RMS\,VE = \sqrt{\frac{1}{N}\sum_{k=1}^{N}\frac{\left(\dot{x}_{true}(k)-\hat{\dot{x}}(k)\right)^2+\left(\dot{y}_{true}(k)-\hat{\dot{y}}(k)\right)^2+\left(\dot{z}_{true}(k)-\hat{\dot{z}}(k)\right)^2}{3}}$$

Root mean square acceleration error:

$$RMS\,AE = \sqrt{\frac{1}{N}\sum_{k=1}^{N}\frac{\left(\ddot{x}_{true}(k)-\hat{\ddot{x}}(k)\right)^2+\left(\ddot{y}_{true}(k)-\hat{\ddot{y}}(k)\right)^2+\left(\ddot{z}_{true}(k)-\hat{\ddot{z}}(k)\right)^2}{3}}$$

(iii) Root sum square position error:

$$RSSPE(k)=\sqrt{(x_{true}(k)-\hat{x}(k))^2+(y_{true}(k)-\hat{y}(k))^2+(z_{true}(k)-\hat{z}(k))^2}$$

Root sum square velocity error:

$$RSSVE(k)=\sqrt{(\dot{x}_{true}(k)-\hat{\dot{x}}(k))^2+(\dot{y}_{true}(k)-\hat{\dot{y}}(k))^2+(\dot{z}_{true}(k)-\hat{\dot{z}}(k))^2}$$

Root sum square acceleration error:

$$RSSAE(k)=\sqrt{(\ddot{x}_{true}(k)-\hat{\ddot{x}}(k))^2+(\ddot{y}_{true}(k)-\hat{\ddot{y}}(k))^2+(\ddot{z}_{true}(k)-\hat{\ddot{z}}(k))^2}$$

(iv) Autocorrelation of residuals with bounds $\pm\frac{1.96}{\sqrt{N}}$ where N is the number of data points

(v) Mode probability which indicates switching from one model to the next

For the present simulated data, following mode transition probability matrices are selected based on the observations made in [8] that large diagonal elements with rows summing to unity will yield near optimal filtering.

(i) For 2-model IMM with CV and CA models, $P_{ij}=\begin{bmatrix}0.99 & 0.01\\ 0.01 & 0.99\end{bmatrix}$

(ii) For 2-model IMM with CV and CJ models, $P_{ij}=\begin{bmatrix}0.99 & 0.01\\ 0.01 & 0.99\end{bmatrix}$

(iii) For 3-model IMM with CV, CA and CJ models, $P_{ij}=\begin{bmatrix}0.99 & 0.001 & 0.009\\ 0.001 & 0.99 & 0.009\\ 0.005 & 0.005 & 0.99\end{bmatrix}$

The process noise covariance selected for the three models are:

$$Q_v=(0.001)^2;\qquad Q_a=(10)^2;\qquad Q_j=(100)^2$$

Figures 4 to 7 shows the comparison of results obtained from all the five cases mentioned in the beginning of this section with the data set 1. The percentage fit error shown in figure 4 indicates that:

(i) EKF with CA and IMM with CV, CA models result in larger PFE since the CA model does not account for the presence of jerk in the data

(ii) EKF with CJ and IMM with CV, CJ models also results in larger PFE values since these models do not properly account for the acceleration in the data

(iii) EKF with CV, CA and CJ models has the lowest PFE since it adaptively estimates all the states during all the regimes of the maneuver

Similar observations follow for the RMS error shown in figure 5.

The RSS error shown in figure 6, which gives the time history of the errors, gives little more insight into what is happening in each case. It can be seen that during the jerk period, the error from EKF with only CA model and IMM with CV and CA models increase because of model inadequacy. During non-maneuvering period EKF with only CJ model shows larger error which indicates that CJ alone may not be sufficient when the target is non-maneuvering and going through constant acceleration motion as well. The 3 model IMM with CV, CA and CJ models shows overall better performance.

Autocorrelation function of residuals of the filter is an indicator of how accurately the model has been able to extract all the information from the given data. Figure 7 shows the comparison of autocorrelation of filter residual plotted along with the bounds for all the cases. It can be observed that the autocorrelation in case of EKF with only CA and IMM with CV and CA are outside the bound indicating the model inadequacy, whereas in case of 3 model IMM, all the autocorrelation values are well within the bounds.

The average mode probabilities estimated from 2-model IMM and 3-model IMM with data set 1 are shown in figures 8 and 9 respectively which indicates the model switching sequence during different regime of trajectory flight. Inclusion of CJ model into the IMM results in low probability being assigned to the CV model during maneuver period.

Figures 10 to 15 show the results corresponding to the data set 2. Figures 10 to 13 show the comparison of results obtained from the different EKF and IMM algorithms. And figures 14 and 15 shows the mode probabilities obtained from 2-model IMM algorithm and 3-model IMM algorithm respectively. From these results similar observation are made that the inclusion of jerk model in the IMM algorithm shows overall better performance of the tracking filter.

6. Concluding Remarks:

A constant jerk model consisting of third order derivative of target position is included in IMM estimator along with constant velocity and constant acceleration models to track a maneuvering target. The motivation for including a higher order model is that agile target maneuvers are likely to have more significant higher order derivatives which lower order tracking models such as constant velocity and constant acceleration models in tracking aplication cannot adequately handle. This has been demonstrated through numerical simulation studies. Inclusion of jerk model in the IMM algorithm shows overall better performance of the tracking filter.

7. References:

1. Girija.G, R. Appavu Raj, J.R. Raol and Kashyap, “Tracking filter and Multi-sensor Data Fusion”, Sadhana, Vol. 29, No.2, pp159-167, 2000.
2. Jatinder Singh, Sudesh K. Kashyap, Girija. G., and J.R. Raol, “Interacting Multiple Model Approach for Target Tracking and Trajectory Estimation”, National Conference on Sensor Technology, Sep. 26-27, 2002, DRDO, Delhi.
3. Yaakov Bar-Shalom and Xiao-Rong Li, “Multitarget-Multisensor Tracking: Principles and Techniques”, 1995.
4. Kishore Mehrotra and Pravas R. Mahapatra, “A Jerk Model for Tracking Highly Maneuvering Targets”, IEEE Trans. on Aero. and Elec. Sys., AES-33, pp 1094-1105, Oct. 1997.
5. Singer R.A., “Estimating Optimal Tracking Filter Performance for Manned Maneuvering Targets”, IEEE Trans. on Aero. and Elec. Sys., AES-7, pp 100-110, Jan. 1970.
6. X. Rong LI and Vesselin P. Jilkov, “Survey of Maneuvering Target Tracking. Part I: Dynamic Models”, IEEE Trans. on Aero. and Elec. Sys., AES-39, pp 1333-1364, Oct. 2003.
7. X. Rong LI and Vesselin P. Jilkov, “Survey of Maneuvering Target Tracking. Part V: Multiple-Model Methods”, Submitted to IEEE Trans. on Aero. and Elec. Sys., Nov. 2003.
8. Bloomer L and Gray J E, “Are more models better?: The effect of the model transition matrix on the IMM filter”, In the southeastern symposium on system theory (SSST), Hentsville, AL, March 2002.

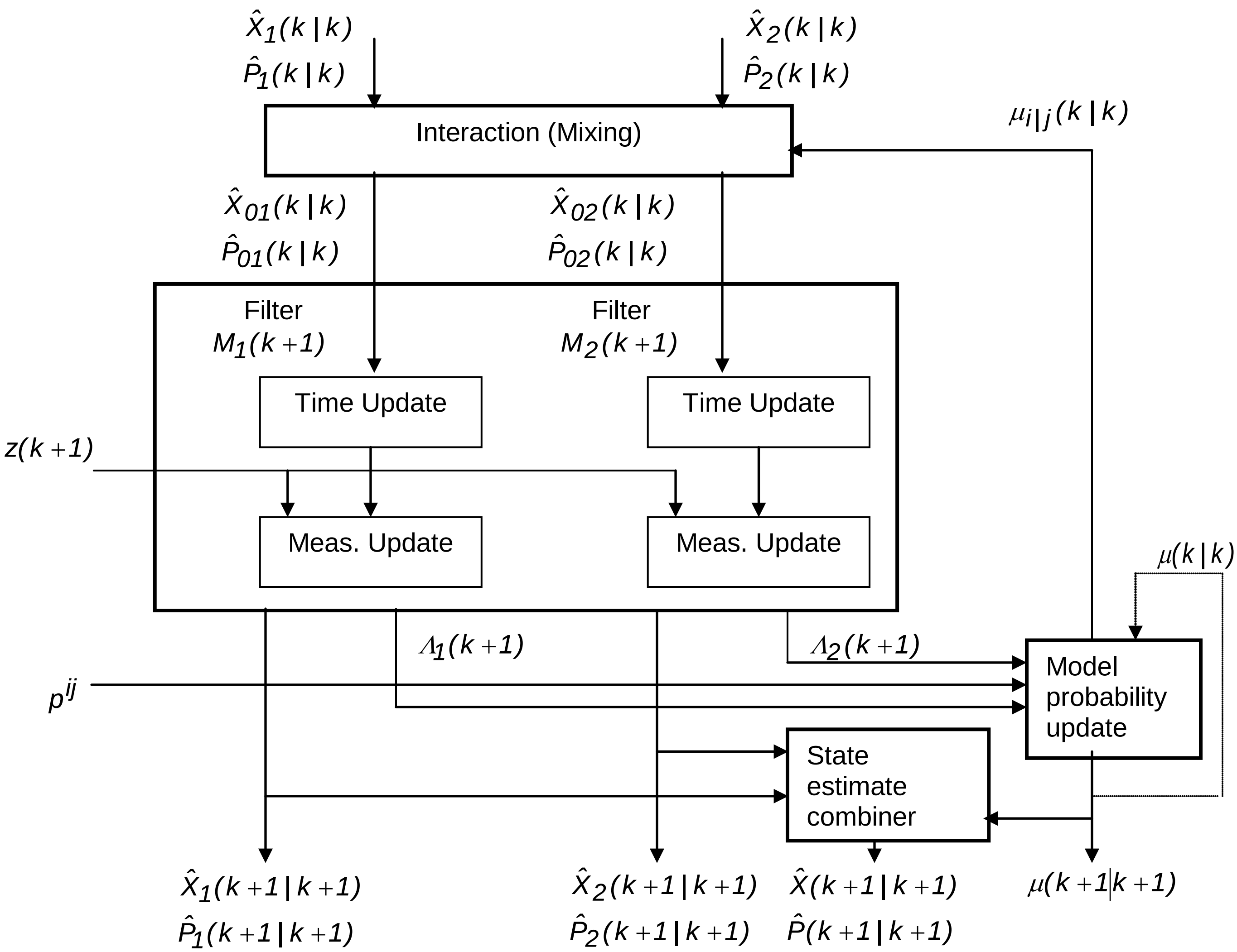

Figure 1: One iteration of two model IMM Kalman filter

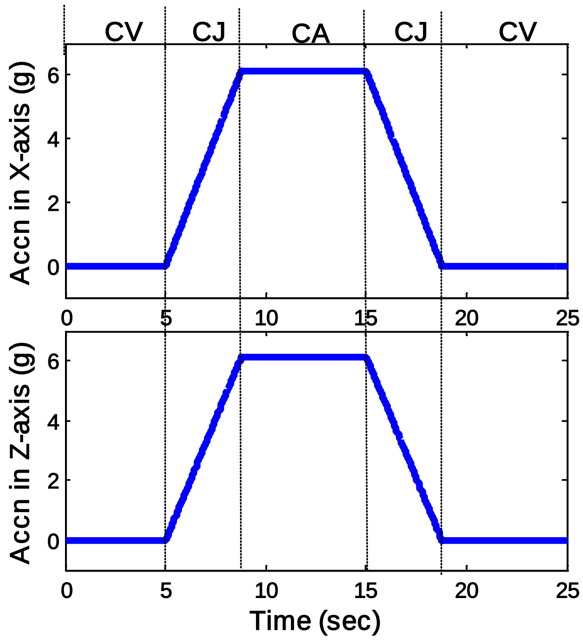

Figure 2(a): Acceleration profile of the target in Cartesian frame (Data Set 1)

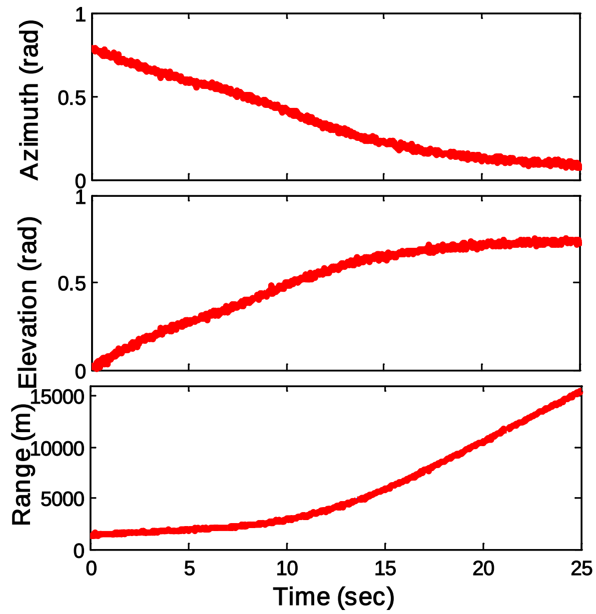

Figure 2(b): Radar tracking measurements (Data Set 1)

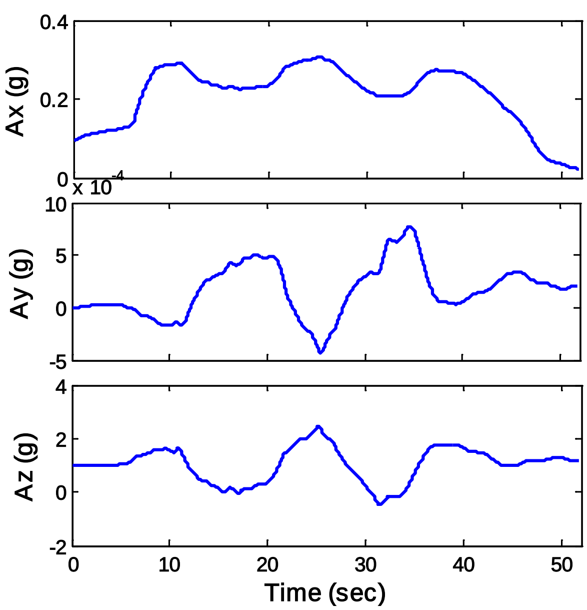

Figure 3(a): Acceleration profile of the target along its body axis (Data Set 2)

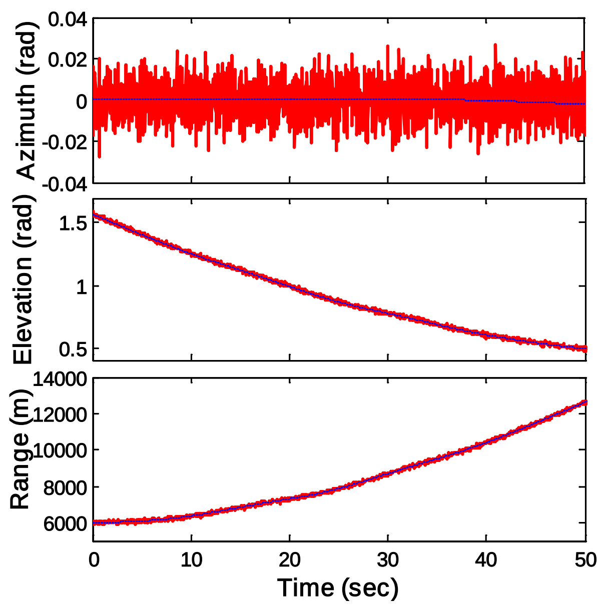

Figure 3(b): Radar tracking measurements (Data Set 2)

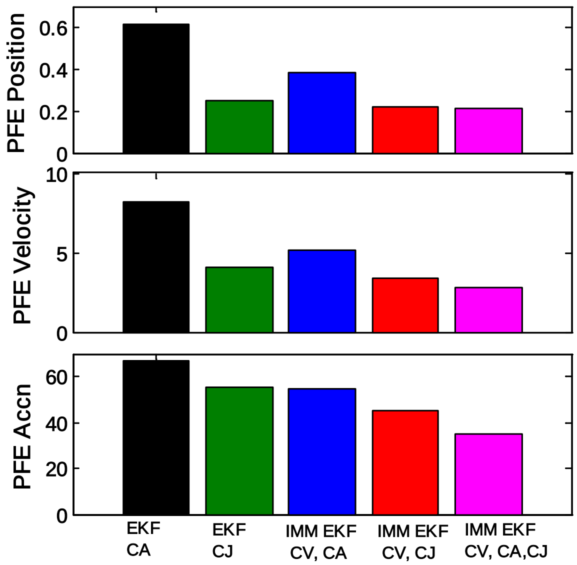

Figure 4: Comparison of percentage fit error in position, velocity and acceleration (Data Set 1)

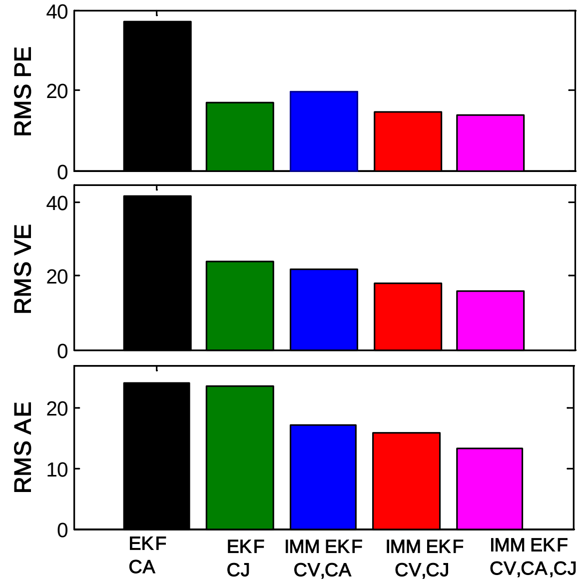

Figure 5: Comparison of RMS position, velocity and acceleration errors (Data Set 1)

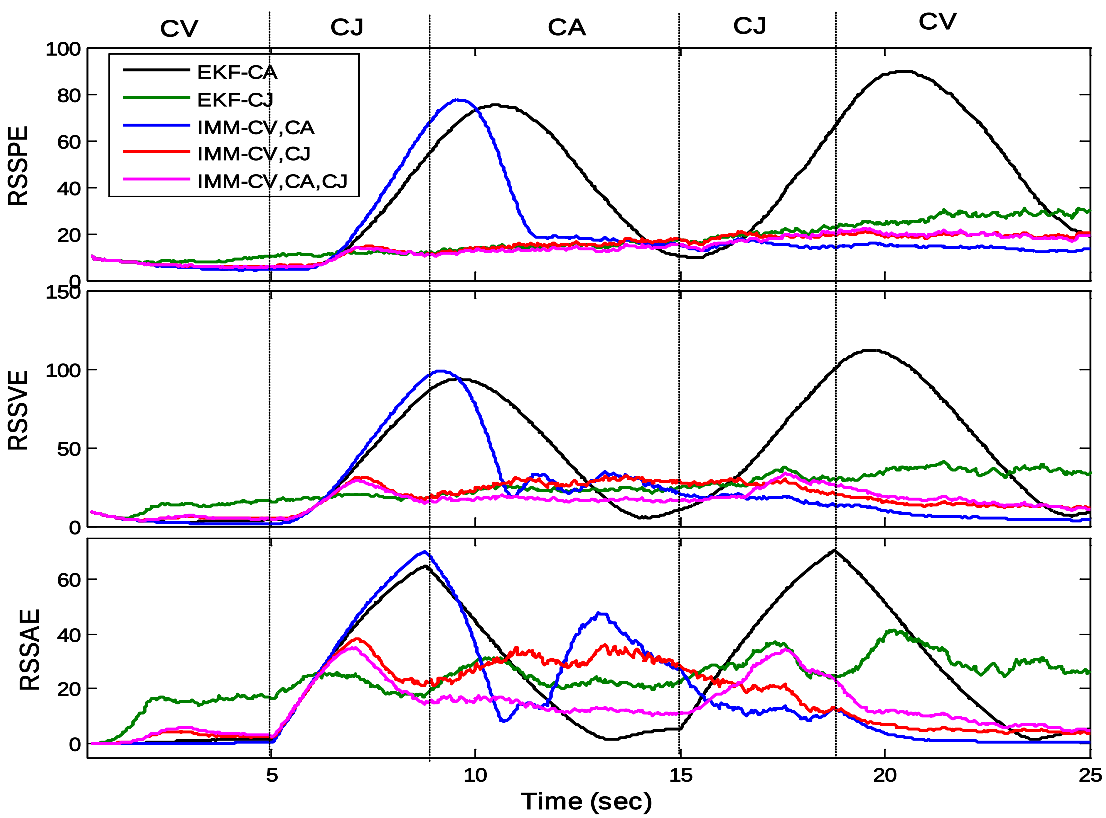

Figure 6: Comparison of RSS position, velocity and acceleration errors (Data Set 1)

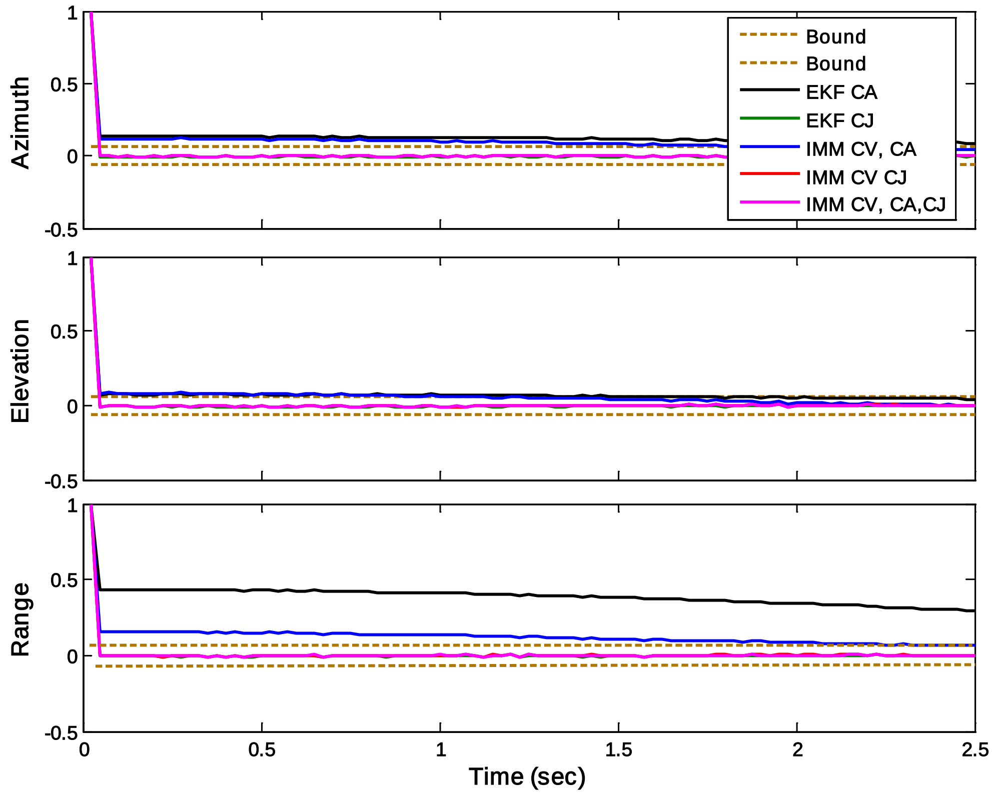

Figure 7: Autocorrelation of filter residual (Data Set 1)

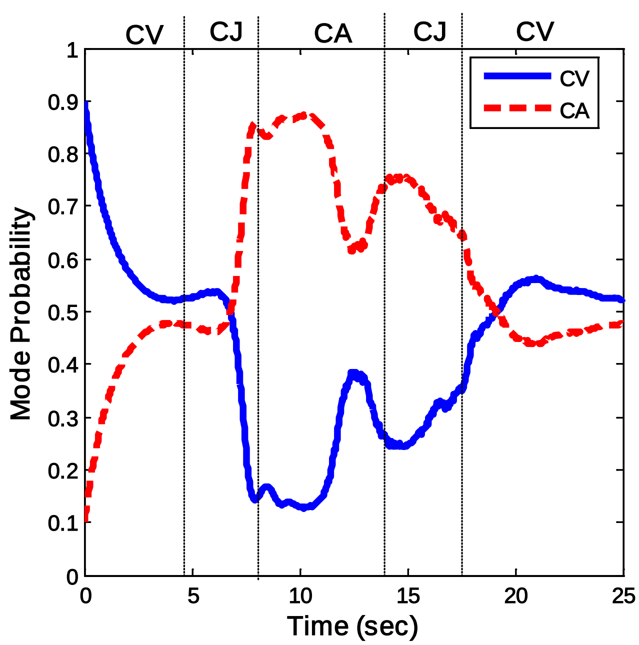

Figure 8: Estimated mode probability in 2-model IMM EKF with CV and CA (Data Set 1)

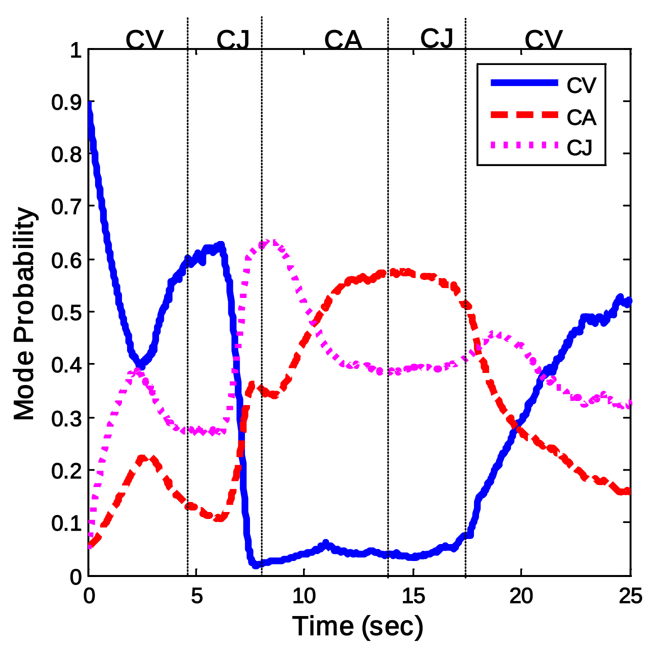

Figure 9: Estimated mode probability in 3-model IMM EKF with CV, CA and CJ (Data Set 1)

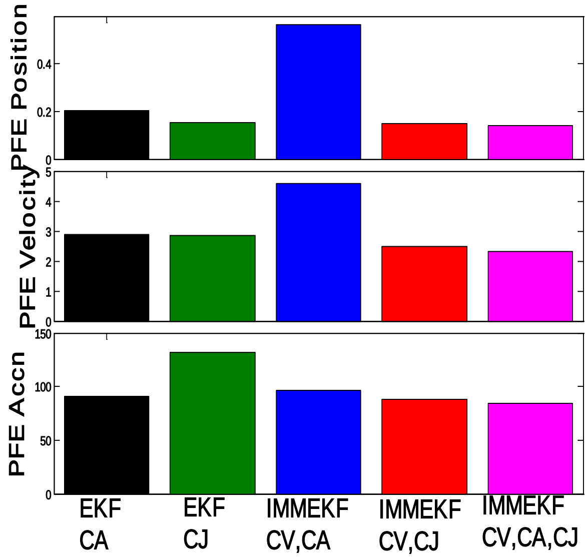

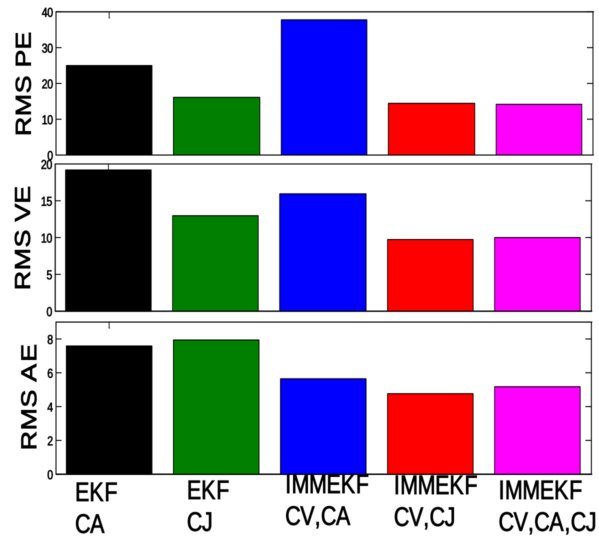

Figure 10: Comparison of percentage fit error in position, velocity and acceleration – Data Set 2

Figure 11: Comparison of RMS position, velocity and acceleration errors – Data Set 2

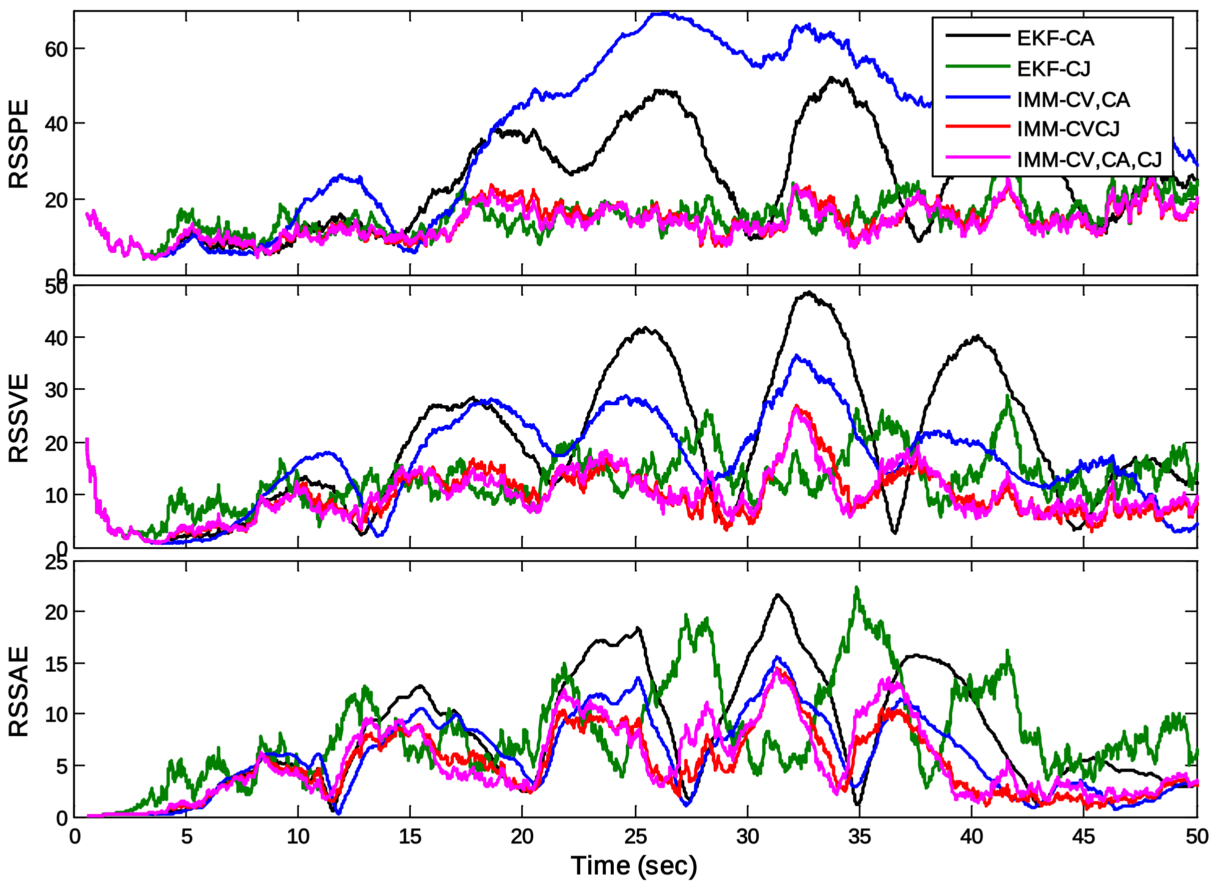

Figure 12: Comparison of RSS position, velocity and acceleration errors – Data Set 2

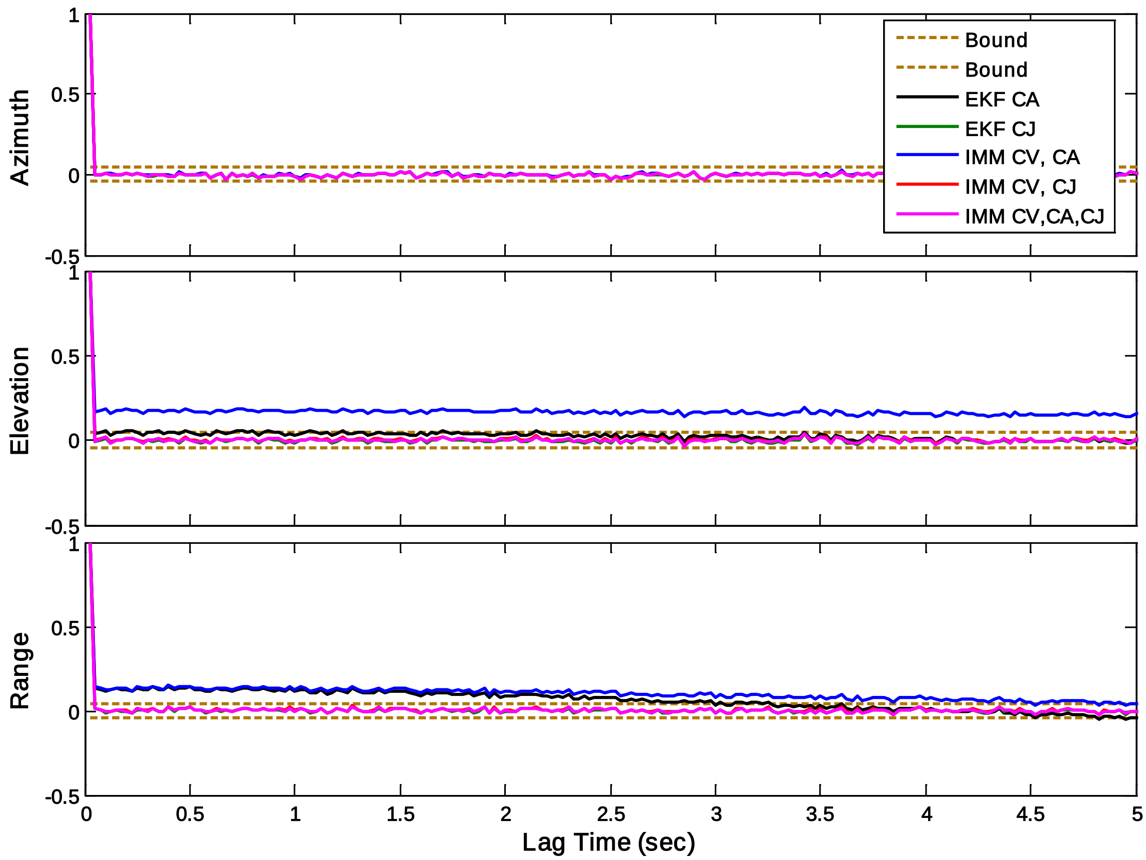

Figure 13: Autocorrelation of filter residual – Data Set 2

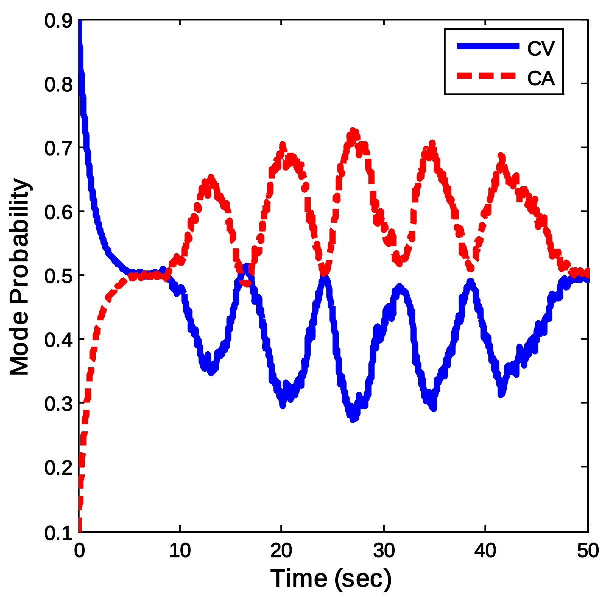

Figure 14: Estimated mode probability in 2-model IMM EKF with CV and CA – Data Set 2

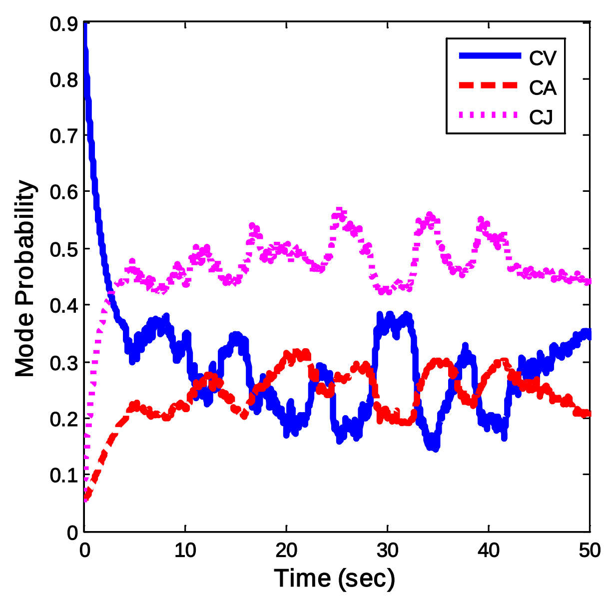

Figure 15: Estimated mode probability in 3-model IMM EKF with CV, CA and CJ – Data Set 2

National Aerospace Laboratories	Classification OPEN No. of copies 8

Title	Three Model IMM-EKF for Tracking Targets Executing Evasive Maneuvers
Author/s	VPS Naidu, Girija G. and Shanthakumar N.

Division	FMCD	NAL Project No.	I-888-1/7
Document No.	PD FC 0701	Date of issue	12 Feb. 2007

Contents	Pages 22 Figures 15 Tables -- References 8
External Participation	------
Sponsor	
Approval	Head, FMCD Group Leader
Remarks	
Keywords	IMM-EKF, Tracking Maneuvering Target, Three Model IMM.

Abstract

A constant jerk model consisting of third order derivative of target position is included in IMM estimator along with constant velocity and constant acceleration models to track a maneuvering target. The motivation for including a higher order model is that agile target maneuvers are likely to have more significant higher order derivatives which lower order tracking models such as constant velocity and constant acceleration models currently in use cannot adequately handle. This has been demonstrated through numerical simulation studies. Inclusion of jerk model in the IMM algorithm shows overall better performance of the tracking filter.